

Production of Synthesis Gas by Direct Catalytic Oxidation of Methane on Pt{110} (1 × 2) Using Supersonic Molecular Beams

A. V. Walker and D. A. King*

Department of Chemistry, University of Cambridge, Lensfield Road, Cambridge, United Kingdom CB2 1EW

Received: February 2, 2000; In Final Form: April 14, 2000

The absolute rate of the methane oxidation reaction over Pt{110} was investigated over the temperature range 400–900 K using molecular beams under ultrahigh vacuum (UHV) conditions. It was found that the surface reaction is biphasic, with CO₂ being the major product at <550 K and CO the major product at >600 K. Under our reaction conditions, the reaction products H₂, CO, and CO₂ were detected. The H₂O production was below the limit of detectability. The product selectivity to CO and CO₂ can be controlled by varying the beam composition as well as the surface temperature. A mean field coupled differential equation model of the process provides a reasonable description of all the experimental observations, although it does not include a proper description of prompt CO desorption at high surface temperatures.

Introduction

In recent years, there has been increased interest in the conversion of methane to synthesis gas (syngas, a mixture of CO and H₂, ideally in a 1:2 ratio). Many industrial processes use syngas as a feedstock; for examples, the Haber process (NH₃ production),¹ methanol synthesis,² and the Fischer–Tropsch process³ (reaction to higher hydrocarbons).

Synthesis gas is usually produced by steam reforming:



To drive this endothermic process, the reactor is heated either externally or internally. In the latter case, heating is achieved by adding O₂ to the feed to provide the energy via highly exothermic combustion reactions. A typical industrial steam reformer operates at 1120–1170 K and 15–30 atm over a Ni/Al₂O₃ catalyst. The CO/H₂ is further adjusted by the water gas shift (WGS) reaction:



Typical WGS reactors operate either at ~470 K using a Cu-based catalyst or at ~670 K using an iron oxide/chromia catalyst. Hence, the conversion of methane to syngas is both expensive and complicated.

An alternative reaction is the direct catalytic partial oxidation of methane to syngas:



This exothermic reaction could not only produce syngas with the ideal ratio for CH₃OH production (if a good catalyst can be found for this process, rather than the steam reforming process using CO₂) or the Fischer–Tropsch process, but it could also lead to the use of smaller and simpler reactors. However, this direct oxidation process is not without its technical difficulties because the reactions to form the secondary oxidation products, H₂O and CO₂, are extremely fast.

Two main proposed reaction mechanisms have been reported in the literature. Prettre et al.⁴ postulated that the reaction

proceeds by conversion to the full oxidation products, H₂O and CO₂, followed by steam reforming, WGS, and CO₂ reforming reactions to the partial oxidation products, CO and H₂. Schmidt et al.^{5,6} observed an almost complete conversion of CH₄ to syngas with a CO selectivity >90% using Pt- and Rh-coated monoliths at short contact times (10⁻³ s) and high spatial velocities (10⁶ h⁻¹). They proposed a second mechanism, a pyrolysis reaction, in which CO and H₂ form first and are subsequently oxidized to H₂O and CO₂.

To elucidate the overall reaction mechanism of the partial oxidation of methane, we conducted a systematic series of studies on Pt{110} (1 × 2) prior to the present investigation that we summarize here. The dissociative sticking probability of O₂ on Pt{110} (1 × 2) is ~0.47 at a surface and thermal beam temperature of 300 K, which is much larger probability than that for CH₄, which is only ~10^{-6–8} at the same temperature. Thus, the rate-determining step is believed to be the dissociative adsorption of methane.

On Pt{110} (1 × 2),⁸ we observed that as the incident translational energy, *E_t*, of the incident methane beam was increased, the initial dissociative sticking probability, *s*₀, passes through a minimum at ~100 meV. At *E_t* > 100 meV, an activated adsorption process becomes dominant, with an activation barrier of ~130 meV. At translational energies >230 meV, *s*₀ attains a limiting value, which is strongly enhanced by the excitation of the C–H stretch modes. We also observed that an increase in surface temperature enhances *s*₀. Two other reaction steps were studied: the interaction of methane with preadsorbed oxygen adatoms, O_a,⁹ and the oxidation of adsorbed carbon.¹⁰

On all surfaces studied to date, Ni{100},¹¹ Ni{111},^{12,13} Pt{111},¹⁴ and Pt{110} (1 × 2),⁹ the initial (zero coverage) dissociative sticking probability of methane, *s*₀, falls with increasing oxygen coverage. We also observed that CO gas was evolved during exposure of the O-precovered surface to the incident CH₄ beam. As the surface temperature is raised to >550 K in the carbon oxidation reaction, there is a switch in selectivity from CO₂ to CO production;¹⁰ the proportion of CO₂ decreases from 95% at *T_s* = 450 K to <1% at *T_s* = 750 K. Using angle-resolved product distribution measurements, we also observed that CO desorbs in a sharp lobe, with an excess translational energy estimated at 135 ± 5 kJ mol⁻¹.

Experimental Section

The experiments were carried out in an ultrahigh vacuum (UHV) chamber¹⁵ equipped with a differentially pumped rotating quadrupole mass spectrometer (QMS), and a stagnation tube and spinning rotor gauge, to measure the beam flux in the molecular beam scattering plane. In an upper level, there is a second QMS, an Ar⁺ sputter gun, and low-energy electron diffraction (LEED) optics.

The sample was a clean single crystal Pt{110} surface orientated to within 1° of the plane and mechanically polished. Initially the surface was cleaned using sputter-anneal cycles and oxygen treatments. Afterward, the surface was cleaned by annealing until a temperature of 1240 K was reached, treating with oxygen while cooling from 1100 to 950 K, and annealing again at 950 K. This procedure yields a clean Pt{110}(1 × 2) surface that exhibits excellent LEED patterns and reproducible temperature-programmed desorption (TPD) spectra for CO¹⁶ and O₂.^{7,17} The sample temperature was monitored using a K-type thermocouple and controlled by a Eurotherm 904P programmable temperature controller.

The CH₄ and O₂ used were >99.9995% and 99.995% pure, respectively, as quoted by the suppliers (Messer UK Ltd.). To increase the translational energy of the CH₄/O₂ mixed beam without increasing the internal energy, it was seeded in He. The translational and internal energy of the CH₄/O₂ mixed beam was also increased by increasing the nozzle temperature. The highest nozzle temperature used was 850 K; we have evidence for methane cracking above 900 K. The translational energy was determined using time-of-flight techniques.

All the reaction products were detected using the fixed QMS. To increase the data collection rate without loss of signal-to-noise, sequential experiments were performed; in the first experiment, only the reaction products CO and CO₂ were followed, and in the second, under the same conditions, the reaction products H₂ and H₂O were recorded. The O₂ and CH₄ beam fluxes were calibrated using a stagnation tube and spinning rotor gauge to quantify the partial pressure rise measured by the QMS. The absolute rate of CO and H₂ produced was also calibrated in a similar way using CO and H₂ beams. To calibrate the CO₂ produced, CO was titrated with a known amount of O_a on the surface and the amount of CO₂ produced was measured. All coverages are quoted as fractional monolayers relative to the number density in the Pt{110} (1 × 1) surface, 9.2 × 10¹⁴ Pt atoms cm⁻².

After the reaction, the sample was oxygen treated at 650 K and then heated to 1200 K at 3 K s⁻¹ to remove any residual C_a present on the surface.

Results and Discussion

Previous studies of CH₄ partial oxidation^{5,6,18} have demonstrated that a number of reaction parameters are important, including the methane-to-oxygen feed ratio and the surface temperature. In the present study, to gain an overall view of the reaction profile, measurements were made of the variation of the reaction products with surface temperature and beam composition. These reactions were then modeled to gain further insights into the reaction mechanism.

At a surface temperature, T_s , of 400 K and a beam energy of 95 meV, the initial (zero coverage) dissociative sticking probability, s_0 , of O₂ is 0.34,⁷ which is 5 orders of magnitude larger than that for CH₄ ($s_0 = 3.4 \times 10^{-6}$)⁸ under the same reaction conditions. However, we note that the value of s_0 for methane increases sharply with increasing surface temperature, incident translational energy, and vibrational energy,⁸ whereas

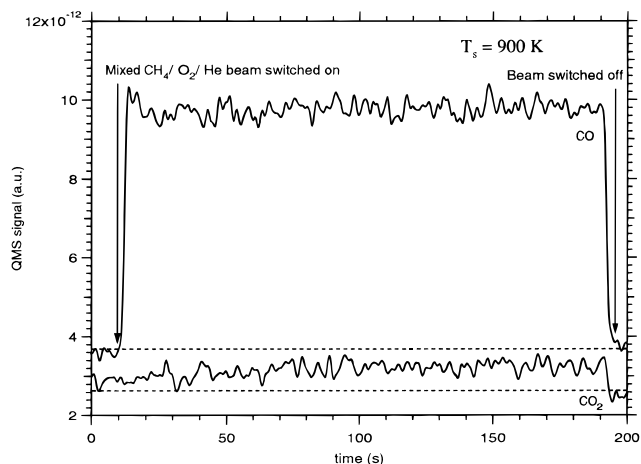


Figure 1. The variation of the rates of production of CO and CO₂ with time at a surface temperature of 900 K. The methane-to-oxygen ratio is 2:1 (effective $p_{\text{CH}_4} = 2 \times 10^{-8}$ mbar). To aid viewing, the CO and CO₂ traces have been vertically displaced. The dotted lines represent the baseline pressures: we note that these are based on more extended ranges of background levels, both before and after beaming, than those shown here.

s_0 for oxygen decreases under the same experimental conditions.⁷ Thus, at a translational energy of 500 meV and nozzle temperature of 800 K, the methane initial sticking probability is ~ 0.01 , whereas the oxygen s_0 decreases to 0.23. Under these reaction conditions, if the CH₄ partial pressure at the sample is 10^{-9} mbar and if all the C_a produced from the dissociative adsorption of methane reacts to form CO and CO₂, it is expected that the total partial pressure rise for the products would be 10^{-11} mbar, which can be easily detected.

The efficiency of formation of each of the reaction products is quoted in terms of a reaction probability, ξ (= product flux/CH₄ flux), which gives the probability that a CH₄ molecule incident on the surface reacts to form that product. The selectivity of the reaction products is also quoted for CO [$s^{\text{CO}} = p(\text{CO})/[p(\text{CO}) + p(\text{CO}_2)]$].

Variation of the Steady-State Products with Surface Temperature and Beam Composition. As the CH₄/O₂/He beam impinges on the clean surface maintained at 900 K (Figure 1), the rate of CO production rises rapidly, followed by a slower rise to a maximum before decreasing to a steady-state value. Thus, the steady-state CO production level is reached after ~ 10 s, whereas the instantaneous level is $\sim 5\%$ higher. Although the noise level on the signal is quite high ($\pm 2.5\%$), the initial higher increase was reproducibly observed. There is a much slower rise in the CO₂ production rate. Because the CO₂ production rate at a crystal temperature of 900 K is very low, the signal-to-noise ratio at steady state is small (~ 2). Nevertheless, an abrupt fall in CO₂ pressure is observed when the beam is terminated (at 193 s in Figure 1), but no abrupt rise is observed when the beam is allowed to impinge on the crystal (at 10 s in Figure 1). Quite clearly, the rate of CO₂ formation rises much more slowly than that for CO.

Isothermal data such as that shown in Figure 1 were obtained at surface temperatures ranging from 900 down to 400 K. (A further example of the data obtained will be presented in Figure 6b.) Steady-state rates of CO and CO₂ production were always achieved within 50 s of allowing the beam to impinge on the crystal. Two factors change as the substrate temperature is lowered. First, the rise in CO production below ~ 600 K is no longer instantaneous, and much less CO is produced. Second, the CO₂ production rate at steady state is significantly increased

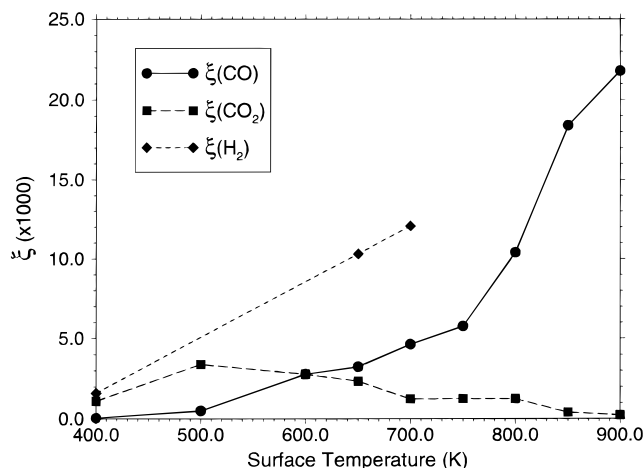


Figure 2. Reaction probability for CO, CO₂, and H₂O formation from a CH₄ + O₂ beam at normal incidence on clean Pt{110}(1 × 2) at various surface temperatures. The methane-to-oxygen ratio is 2:1 (the stoichiometric ratio for CO production).

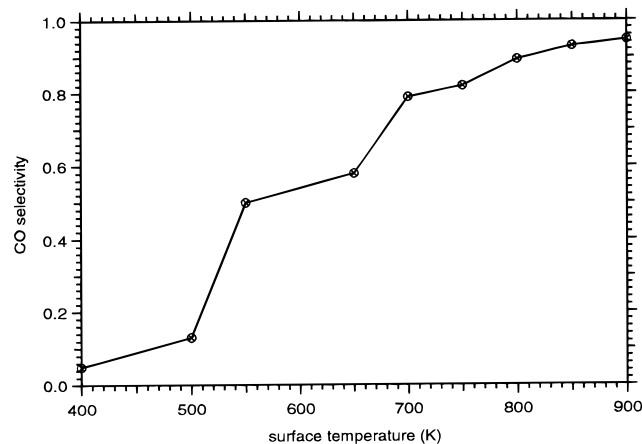


Figure 3. Selectivity to CO formation from a CH₄ + O₂ beam at normal incidence on clean Pt{110}(1 × 2) at various surface temperatures. The methane-to-oxygen ratio is 2:1 (the stoichiometric ratio).

and, as a function of time after switching on the reactants, it shows a pronounced maximum before decaying to the steady-state rate of CO₂ production. Figure 2 displays ξ for the formation of the products CO, CO₂, and H₂ at steady state for a methane-to-oxygen ratio of 2:1 (the stoichiometric ratio for the partial reaction to CO) at various surface temperatures, T_s . Under the reaction conditions used, no water formation was detected at any surface temperature (or beam composition) measured, which is surprising because the H₂O formation reaction from H and O adatoms is fast at room temperature and above.¹⁹ However, after the work described in the present paper Watson, van Dijk, and King²⁰ were able to study the reaction at incident methane fluxes ~ 10 times higher than those described in the present work. In this way, H₂O production was observed, with the selectivity being dependent on both the surface temperature and the CH₄:O₂ ratio in the beam. We therefore conclude that the inability to detect H₂O production in the present work arose from the relative insensitivity to H₂O detection.

As the surface temperature is raised from 400 to 900 K, the selectivity switches from CO₂ to CO (Figure 3). At 400 K, the CO selectivity is 4%, but at 900 K it is 95%. This behavior is similar to that observed for the reaction of pre-adsorbed C and

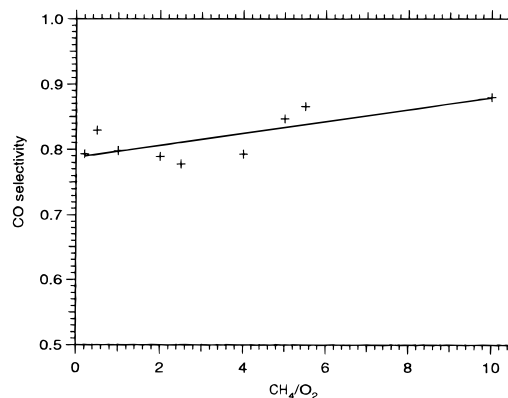


Figure 4. Selectivity to CO formation from a CH₄ + O₂ beam at normal incidence on clean Pt{110}(1 × 2) at various beam compositions at a surface temperature of 700 K.

O₂.¹⁰ Hence, we conclude that the same reaction is dominant. It was demonstrated that CO formed in the surface reaction at high temperatures desorbs with excess energy of 135 ± 5 kJ mol⁻¹; a detailed discussion of the mechanism is given elsewhere.¹⁰ There is a sharp rise in CO selectivity at ~ 700 K. At low coverages, O₂ desorbs at ~ 700 K, and this loss of surface oxygen adatoms is associated with the fall in CO₂ production at these temperatures. We note that at a surface temperature of 400 K, the selectivity to CO (0.05) is higher than that observed for the oxidation of preadsorbed C [$s(\text{CO}) = 0.02$].¹⁴ Very recently, Watson et al.²¹ have shown that at temperatures below ~ 500 K, the stable product of methane dissociation is methyne (CH). The reaction with O₂ at these temperatures proceeds through a new pathway involving CH, and not adsorbed C. The rate of the reaction of O₂ with C at 400 K is negligible compared with this new reaction with CH.²⁰

Figure 4 shows the selectivity to CO for various beam compositions at a surface temperature of 700 K. As the CH₄-to-O₂ ratio changes from 1:2 to 10:1, the CO selectivity increases somewhat from $\sim 79\%$ at a ratio of 1:5 to 88% at a ratio of 10:1. These observations are also reminiscent of the variation of CO selectivity with incident O₂ beam flux measured for C_a oxidation.¹⁰

Temporal Evolution of the Products. The formation rate of CO was always observed to rise very rapidly, before the CO₂ production rate (Figure 1), and we conclude from the temporal evolution of CO and CO₂ that the reaction mechanism is similar to that observed for C_a oxidation.¹⁰ At surface temperatures below ~ 650 K, the rate of CO₂ formation also passes through a maximum, whereas at higher temperatures, the CO₂ formation rate rises slowly. Oxygen slows down the dissociative adsorption of methane;⁹ as the reaction progresses, the methane dissociative sticking probability, and hence the rate of C_a formation, decreases to a steady-state value. Thus, the rates of CO and CO₂ formation are observed to pass through maxima. At higher surface temperatures, the net dissociative sticking probability is lower and O₂ desorption occurs, producing a lower O_a coverage. The dissociative sticking probability of methane therefore remains higher and the maximum in the rate of CO and CO₂ production is less pronounced (Figure 1).

Mathematical Model

To obtain further insights into the experimental observations and to test the hypothesis that the dominant mechanism to form CO and CO₂ is C_a oxidation, the reaction was modeled using a

mean-field approximation based on the following elementary processes:



where the subscripts a and g denote an adsorbed surface and a gaseous species, respectively. Equations 1 and 2 represent the dissociative adsorption of methane and oxygen. The dissociative adsorption of methane to form carbon and hydrogen adatoms is treated as a direct activated process.⁸ The presence of the reaction products on the surface are only considered for H₂ and CO because CO₂ and H₂O have a very short lifetime in this temperature range. We note that this simple Langmuir–Hinshelwood formulation, in which all surface species and gaseous products are assumed to be equilibrated to the surface temperature, does not describe the reaction to form hot CO via a [C–O–O][±] intermediate.¹⁰ However, hot CO is only formed at the highest surface temperatures used. At intermediate temperatures, equilibrated CO is formed, and this is appropriately described by the Langmuir–Hinshelwood formulation. Similar considerations and reservations apply to our mean-field modeling of the reaction of O₂ with preadsorbed carbon.¹⁰ Nevertheless the formalism provides a relatively simple way forward.

All reactions take place on the (1 × 2) phase because the adsorption of oxygen has been shown not to induce the lifting of the (1 × 2) surface reconstruction to the (1 × 1) phase;⁷ the CO coverage on the surface under the conditions described is always extremely small, ≪0.01 mL, and is therefore too low to induce the lifting of the (1 × 2) reconstruction.¹⁶ Even at temperatures below the desorption temperature of CO, a low coverage is maintained because of the reaction with adsorbed oxygen to form CO₂.

A set of four coupled differential equations is used to describe the variations in the adsorbate coverages (θ_C, θ_O, θ_{CO}, and θ_H) on the surface. All coverages are quoted relative to the Pt atom density in the ideal (1 × 1) surface. Sticking probabilities for each gas are denoted by s_{gas}:

$$\frac{d\theta_C}{dt} = k_1 s_{\text{CH}_4} P_{\text{CH}_4} - k_3 \theta_C \theta_O \quad (\text{A})$$

$$\frac{d\theta_O}{dt} = k_2 s_{\text{O}_2} P_{\text{O}_2} - k_3 \theta_C \theta_O - k_4 \theta_{\text{CO}} \theta_O - k_6 \theta_H \theta_O \quad (\text{B})$$

$$\frac{d\theta_{\text{CO}}}{dt} = k_3 \theta_C \theta_O - k_4 \theta_{\text{CO}} \theta_O - k_5 \theta_{\text{CO}} \quad (\text{C})$$

$$\frac{d\theta_H}{dt} = 4k_1 s_{\text{CH}_4} P_{\text{CH}_4} - 2k_6 \theta_H \theta_O - k_7 (\theta_H)^2 \quad (\text{D})$$

Variations in θ_C are described in eq A, which contains adsorption (k₁) and reaction to form CO_a (k₃). The variation of the

TABLE 1: Reaction Parameters Used in the Model

reaction	rate (s ⁻¹)	E _a (kJ mol ⁻¹)	ν (s ⁻¹)	ref
CH ₄ impingement rate	k ₁	4.155 × 10 ⁵ ML mbar s ⁻¹		calc.
O ₂ impingement rate	k ₂	2.938 × 10 ⁵ ML mbar s ⁻¹		calc.
C _a + O _a → CO _a	k ₃	0	24	10
CO _a + O _a → CO ₂ (g)	k ₄	58.6	2 × 10 ⁹	25, 26
CO _a → CO (g)	k ₅	158.8	2 × 10 ¹⁶	16, 26
2H _a + O _a → H ₂ O (g)	k ₆	54.4	1 × 10 ¹³	23, 24
2H _a → H ₂ (g)	k ₇	E(θ = 0) = 54.8 α = 10.5 kJ mol ⁻¹ mL ⁻¹	3 × 10 ¹¹	26

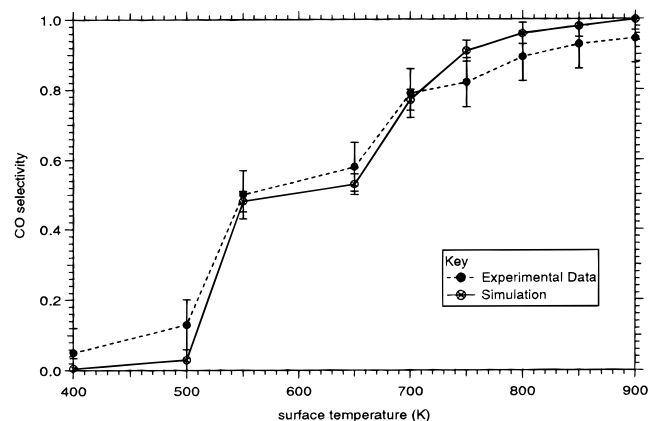


Figure 5. Selectivity to CO formation from the model simulations for the reaction of CH₄ + O₂ in a 2:1 ratio (effective p_{CH₄} = 2 × 10⁻⁸ mbar) at various surface temperatures. The experimental observations are also shown for comparison.

dissociative sticking probability, s_{CH₄} with oxygen adatom coverage has been measured under the same experimental conditions.⁹ The sticking probability also varies with carbon coverage,⁸ but this variation is ignored because the carbon coverage is expected to remain very low. The rate constant k₃ used is taken from ref 10.

Equation B describes the variation in oxygen coverage due to adsorption (k₂) and the reactions to form CO (k₃), CO₂ (k₄), and water (k₅). We note that the sticking probability s_{O₂} is a net sticking probability. The same rate constants, k₄ and k₅, are used as in earlier modeling of NO + H₂,^{22,23} CO + O₂,²⁴ and NO + CO.²⁵ Similarly, eq C describes the variation of CO coverage due to formation (k₃) and removal by either reaction to CO₂ (k₄) or desorption (k₅). During the experiment, θ_{CO} is expected to remain extremely low and the desorption energy was therefore assumed to remain constant.

The variation of θ_H is described by eq D. The processes involved are methane dissociative adsorption (k₁), reaction to H₂O (k₆), and desorption (k₇). The data were fitted with a desorption energy of the form E_d = E_d(θ = 0 mL) - αθ, where α is an interaction energy between neighboring H adatoms.

The differential equations were integrated numerically using the fourth-order Runge Kutta formula²⁷ with time between 5 × 10⁻⁷ and 1 × 10⁻⁴ s. The parameters used are listed in Table 1.

Variation of the Product Distribution with Surface Temperature. Without further fitting or alteration of any of the literature parameters, the model was found to have a very high selectivity to H₂O, which increased from 69% at 400 K to 77% at 900 K. Under our present low CH₄ incident beam flux conditions, we were unable to detect the H₂O formed, and this prediction could not be confirmed. Excellent agreement with the observed experimental CO selectivities is, however, obtained for surface temperatures between 400 and 900 K (Figure 5).

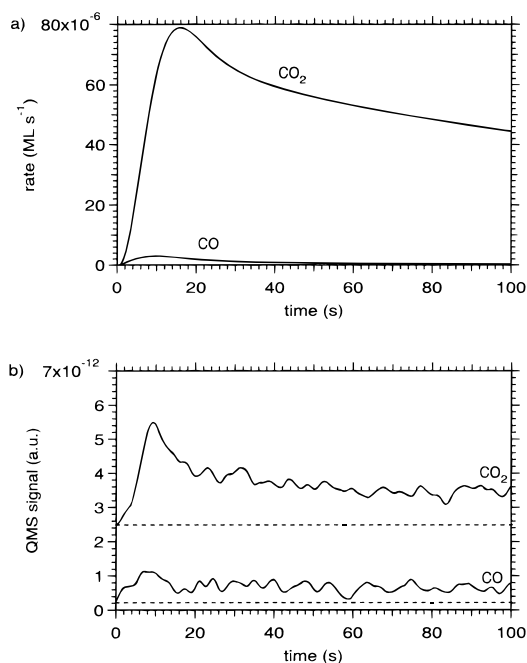


Figure 6. The variation of simulated rates of production of CO and CO₂ with time at a surface temperature of 500 K. The methane-to-oxygen ratio is 2:1 (effective $p_{\text{CH}_4} = 2 \times 10^{-8}$ mbar): (a) model; (b) experimental results. The dotted lines indicate the baseline pressures.

Temporal Evolution of the Reaction Products. Using the model, we have computed the temporal evolution of the products. In qualitative agreement with experiment, as soon as the mixed CH₄/O₂/He beam impinges upon the surface ($t = 0$ s), there is an increase in the rate of production of CO that rises to a maximum before decreasing to a steady-state value (Figure 6). However, the increase in production rate is not as fast as that observed experimentally. This initial increase is followed by a slower rise in the CO₂ production rate. At surface temperatures <650 K, the computed CO₂ production rate goes through a maximum. The model does predict maxima at longer times than is experimentally observed, particularly for CO₂ production. However, the experimentally observed trends are reproduced. Also in agreement with experiment, at temperatures <650 K, there is a slow build up of the CO₂ production rate. At all surface temperatures measured, the computed C coverage passes through a maximum 10–15 s before sharply dropping to a steady-state value as the oxygen adatom coverage increases; as previously noted, oxygen poisons the surface to the dissociative adsorption of methane.¹³ The maximum in the carbon coverage approximately coincides with the maximum in the CO production rate. Hence, during the first part of the reaction, the CO formation rate is controlled by the amount of carbon present on the surface. The carbon coverage at the temporal peak decreases with increasing T_s , which in turn corresponds to a less pronounced CO production rate peak.

Under the conditions of the reaction, the modeling shows that the coverage in oxygen adatoms varies over the range 0.2–0.1 ML in the temperature range 500–850 K. Over the same temperature range, the carbon adatom coverage varies between 0.007 and 0.0045 ML.

Reaction Mechanism

Product selectivity in the methane oxidation reaction over Pt{110}(1 × 2) is controlled by the parameters of surface temperature and surface oxygen coverage. The experimental observations can be explained within a model that considers

the competition between CO desorption and reaction to CO₂ as a function of surface temperature and surface oxygen coverage.

The proposed mechanism is a direct oxidation process and has some similarities to the mechanism proposed by Schmidt and co-workers.^{5,6} It can be broken down into a series of steps. Steps 1 and 2 describe methane and oxygen dissociative adsorption.



At surface temperatures above ~550 K, methyl, formed from the dissociative adsorption of methane, rapidly dehydrogenates to C_a and H_a.^{28,29} Thus, all reactions occur on the surface between carbon, oxygen, and hydrogen adatoms.

The experimental observations indicate that the oxygen adatom coverage is important. As θ_{O} increases, there is a decrease in the dissociative sticking probability of methane¹³ and hence in the rate of C production.

The CO formation rate rises almost instantaneously as the mixed CH₄ + O₂ beam impinges on the surface, followed by a slower rise. After a measurable delay, the rate of CO₂ production increases. Thus, the dominant reaction mechanism for the production of CO and CO₂ is similar to that observed for C_a oxidation;¹⁸ we conclude that a significant proportion of CO desorbs from the surface translationally and vibrationally hot at high surface temperatures.

As the surface temperature is increased, the selectivity to CO and the reaction probability, ξ (CO), increases. The increase in ξ reflects an increase in the dissociative sticking probability of methane with surface temperature, T_s , whereas the concomitant decrease in ξ (CO₂) is associated with a decrease in steady-state O_a coverage with increasing T_s and the increasing propensity for prompt (hot) CO to form. At a surface temperature of 900 K and a methane-to-oxygen ratio of 2:1 (the stoichiometric ratio for CO production), the CO selectivity is 95%.

Summary

In using a molecular beam gas source for a mechanistic study of catalytic reactions, where a high pumping speed is maintained in the reaction chamber, the reaction is uniquely examined under the condition of single collisions of each reacting molecule with the surface and effectively *no* collisions of product molecules with the surface. In the present work we have demonstrated, for the first time, that under these conditions, the continuous reaction between CH₄ and O₂ to the products CO, CO₂, and H₂ can be studied. The results clearly show no support for the reaction mechanism suggested many years ago by Prettre et al.,⁴ invoking complete oxidation to gaseous CO₂ and H₂O in the first step and subsequent formation of CO and H₂ by reactive collisions of the initial gaseous products with the surface. Similarly, our results show the biphasic nature of the surface reaction, without invoking gaseous CO production in a first step, followed by CO₂ formation when CO is readsorbed. Instead, we have shown that the product selectivity to gaseous CO or CO₂ is entirely determined by surface processes, and is very strongly dependent on surface temperature, and to a lesser extent on the CH₄:O₂ ratio.

The results are largely consistent with our earlier study¹⁰ of the interaction of gaseous O₂ with preadsorbed carbon, formed by the decomposition of methane at surface temperatures <500 K. At the highest surface temperatures (≥650 K), gaseous CO is formed via a prompt process assigned to the explosive

decomposition of a surface intermediate formed between chemisorbed molecular O₂ and adsorbed C: this hot CO, with an equivalent temperature of ~11,000 K,¹⁰ would need to be accounted for in the modeling of the reaction in a standard catalytic reactor. As the surface temperature is lowered, two new factors come into play. First, the hot CO released onto the potential energy surface for chemisorbed CO by decomposition of the O₂C reaction intermediate exchanges energy with the surface, as the surface temperature is lowered to <650 K, and becomes thermally accommodated to the surface: it can subsequently desorb as CO or react with adsorbed O to form CO₂. Second, the surface reaction between O and C adatoms becomes more effective in the production of adsorbed, thermally equilibrated CO; as the temperature is lowered, the CO lifetime on the surface increases, the reaction with adsorbed O takes over, and the dominant product becomes CO₂.

One important difference with our previous study of O₂ interacting with preadsorbed C is noted. At temperatures between 350 and 400 K, the stable surface species formed from methane dissociation is CH.²¹ Watson et al.²⁰ have shown that this CH species, at low surface temperatures, is more reactive to coadsorbed O_a than C. This alternative reaction pathway has not been accounted for in the present work.

We have formulated a Langmuir–Hinshelwood mechanism, using a mean-field approach, to model the reaction. Although the model provides a good description of the steady-state selectivity of the reaction to CO or CO₂ and the overall reaction probability and a reasonably good description of the temporal evolution of the products, it has its limitations. In particular, the model does not account for the production of prompt CO, nor does it account, in its present form, for the presence of CH on the surface.

Acknowledgment. We acknowledge EPSRC for an equipment grant, Shell Research and Technology Centre, Amsterdam, for a studentship (A.V.W), and support from and discussions with Professor Gert Jan Kramer.

References and Notes

- (1) Stacey, M. H. *Catalysis* (London) **1990**, 3, 1998.
- (2) Kang, H. H. *Catal. Rev. Sci. Eng.* **1981**, 22, 235.
- (3) Fischer, F.; Tropsch, H. *Brennst.-Chem.* **1926**, 7, 197; *Chem. Ber.* **1926**, 59, 830.
- (4) Prettre, M.; Eichner, C.; Perri, M. *Trans. Faraday Soc.* **1946**, 43, 335.
- (5) Tornianen, P. M.; Chu, X.; Schmidt, L. D. *J. Catal.* **1994**, 146, 1.
- (6) Hickman, D. A.; Schmidt, L. D. *ACS Symposium Series* **1993**, 523, 416; *Aiche* **1993**, 39, 1164; *Science* **1993**, 259, 343.
- (7) Walker, A. V.; Klötzer, B.; King, D. A. *J. Chem. Phys.* **1998**, 109, 6879.
- (8) Walker, A. V.; King, D. A. *Phys. Rev. Lett.* **1999**, 82, 5156.
- (9) Walker, A. V.; King, D. A. *Surf. Sci.* **2000**, 444, 1.
- (10) Walker, A. V.; King, D. A. *J. Chem. Phys.* **2000**, 112, 1937.
- (11) Quinlan, M. A.; Wood, B. J.; Wise, H. *Chem. Phys. Lett.* **1985**, 118, 478.
- (12) Krishnan, G.; Wise, H. *Appl. Surf. Sci.* **1989**, 37, 244.
- (13) Alstrup, I.; Chorkendorff, I.; Ullmann, S. *Surf. Sci.* **1990**, 234, 79.
- (14) Valden, M.; Xiang, N.; Pere, J.; Pessa, M. *Appl. Surf. Sci.* **1996**, 99, 83.
- (15) Hopkinson, A.; Guo, X.-C.; Bradley, J. M. *J. Chem. Phys.* **1993**, 99, 8262.
- (16) Hoffmann, P.; Bare, S. R.; King, D. A. *Surf. Sci.* **1982**, 117, 245.
- (17) Wilf, M.; Dawson, P. T. *Surf. Sci.* **1977**, 65, 399.
- (18) Lee, J. H.; Trimm, D. L. *Fuel Proc. Technol.* **1995**, 42, 339.
- (19) Hellsing, B.; Kasemo, B.; Zhdanov, V. P. *J. Catal.* **1991**, 132, 210.
- (20) Watson, D. T. P.; van Dijk, J.; Harris, J.; King, D. A., to be published.
- (21) Watson, D. T. P.; Titmuss, S.; King, D. A., submitted for publication.
- (22) Lombardo, J.; Fink, T.; Imbihl, R. *J. Chem. Phys.* **1993**, 98, 5526.
- (23) Gruyters, M.; Pasteur, A. T.; King, D. A. *J. Chem. Soc., Faraday Trans.* **1996**, 92, 2941.
- (24) Gruyters, M.; Ali, T.; King, D. A. *J. Phys. Chem.* **1996**, 100, 14417.
- (25) Hopkinson, A.; King, D. A. *Chem. Phys.* **1993**, 177, 433.
- (26) McCabe, R. W.; Schmidt, L. D. *Surf. Sci.* **1976**, 60, 85.
- (27) *Numerical Recipes in C: the Art of Scientific Computing*, 2nd Ed.; Press, W. H.; Teukolsky, S. A.; Vetterling, W. T.; Flannery, B. P., Eds.; Cambridge University Press: New York, 1992; p 710.
- (28) Oakes, D. J.; Newell, H. E.; Rutten, F. J. M.; McCoustra, M. R. S.; Chesters, M. A. *J. Vac. Sci. Technol. A* **1996**, 14, 1439.
- (29) Zaera, F.; Hoffmann, H. *J. Phys. Chem.* **1991**, 95, 6397.